

Corrosion Inhibitors and Effect of Various Mechanical Processes on Material Corrosion

Nikhil S. Deshmukh¹, Dr Purushottam Desale²

¹SSVPS, B.S.Deore, College of Engineering, Dhule, MS, 424005, India

²SSVPS, B.S.Deore, College of Engineering, Dhule, MS, 424005, India

Abstract

Corrosion is serious problem, causing direct and indirect losses. Complete elimination of corrosion of metals is not achieved till date. But by implementing certain methods it can be controlled up to certain level. Various corrosion inhibitors are in used nowadays and every new day a blend of corrosion inhibitor is in development presently. The paper discusses about inhibitors in various forms like natural inhibitors, chemical inhibitors and effect of various mechanical processes on corrosion behavior of metals. Various inhibitors with their particular application is discussed in brief stating their effects on characterization of material and effectiveness as inhibitors.

Keywords: Corrosion; Chemical inhibitors; Mechanical processes; Material Characterization; Natural inhibitors

1. INTRODUCTION

Corrosion is generally determination of metal surface mainly because of chemical and electrochemical reactions. The rate of corrosion is depends on types on metal and surrounding conditions. Also though metal is same but surface properties are different then it is observed that the rate of corrosion changes considerably in the medium.

1.1 Types of Corrosion

The main general types of corrosion are general attack corrosion , localized, galvanic and environmental corrosion. In General Attack Corrosion, corrosion attacks the entire surface of a metal structure. It is caused by chemical or electrochemical reactions. While general attack corrosion can cause a metal to fail, it is also a known and predictable issue. SO it is possible to control it easily than other corrossions



Fig.1 General Corrosion on Mechanical Parts

(Referred From: <https://moontanks.com/is-corrosion-eating-into-your-bottom-line/>)

Localized corrosion attacks only portions of a metal structure. It may be classified as Pitting which causes the creation of small holes in the surface of a metal, Crevice corrosion that occurs in stagnant locations such as those found under gaskets. And filiform corrosion that occurs when water gets under a coating such as paint.



Fig.2 Localised corrosion.

(Referred From: <https://www.montanstahl.com/blog/corrosion-on-stainless-steel/>)

Galvanic corrosion generally occurs at electrochemical liquid solution material, here corrosion of only one of two metals takes place due to molecular reaction.

1.2 Losses Due to Corrosion

It is seen that corrosion is making direct and indirect losses such as direct losses are termed as cost of replacing, cost of repainting, maintenance while indirect losses can be summed up as shutdown, loss of product, loss of efficiency, contamination of product, overdesigning of equipments etc.

According to the world corrosion organization corrosion causes US 2.5 trillion dollars globally (approximately 17,80,87,50,00,00,000 Indian Rupee). Also the costs the loss of life and jobs. The 20-25% of this can be eliminated by corrosion prevention techniques. Corrosion prevention should not be considered for just a financial aspect but for health and safety aspect also.

1.3 Methods of Corrosion Control

Some simple methods include correction of environment factors such as controlling parameters of environmental conditions like feed water for water boilers can be treated with softeners or other chemical media to adjust the hardness, alkalinity and or oxygen content in order to reduce corrosion on the interior of the unit.

Surface conditions is one of the parameter in prevention of corrosion. As the single material is not corrosion resistant in all the environments but once the correct metal is chosen the role of metallurgical conditions comes into picture. Because the similar metal shows different corrosion behavior in same environment when it is processed with varying machining parameters.

Corrosion inhibitors, coating, plating etc are also corrosion prevention methods in which corrosion inhibitors are chemicals that react with the metal's surface or the environmental gasses, thereby interrupting the chemical reaction that causes corrosion. Paints and other organic coatings are used to protect metals from the degradative effect of environmental gasses.

Metallic coatings, or plating, can be applied to inhibit corrosion as well as provide decorative finishes.

There are four common types of metallic coatings:

Electroplating: A thin layer of metal - often nickel, tin, or chromium - is deposited on the substrate metal (generally steel) in an electrolytic bath. The electrolyte usually consists of a water solution containing salts of the metal to be deposited.

Mechanical plating: Metal powder can be cold welded to a substrate metal by tumbling the part, along with the powder and glass beads, in a treated aqueous solution. Mechanical plating is often used to apply zinc or cadmium to small metal parts.

Electrolyses: A coating metal, such as cobalt or nickel, is deposited on the substrate metal using a chemical reaction in this non-electric plating method.

Hot dipping: When immersed in a molten bath of the protective, coating metal a thin layer adheres to the substrate metal.

2. LITERATURE REVIEW

Extensive work is going on with corrosion inhibitors. The effective methods of corrosion prohibitions

are mainly natural corrosion prohibitory, chemical corrosion inhibitors and effect of mechanical process on corrosion behavior of material.

M. Esmaily, M. Shahabi-Navid, J.-E. Svensson, M. Halvarsson, L. Nyborg, Y. Cao, L.-G. Johansson considered the parameter in corrosion control as temperature. Authors discussed the effect of temperature on the NaCl-induced atmospheric corrosion of the Mg–Al alloy AM50. The authors are come up with results that the NaCl-induced atmospheric corrosion of AM50 is strongly reduced with decreasing temperature, 99.97% Mg does not exhibit such a trend. Also the finding was that several crystalline magnesium hydroxyl carbonates formed at 4 and 22 C but were absent at -4 C. Also authors concluded with the temperature dependence of the corrosion of alloy AM50 is tentatively attributed to its aluminum content and the increased

inhibitive effect of CO₂ at low temperature is suggested to be due to an increased solubility of CO₂ in the aqueous electrolyte at low temperature.[1]

A. Banos, C.P. Jones, T.B. Scott come up with the effect of mechanical process parameter and its effect on material characteristics which has affected the corrosion rate. From their analysis found that heat treatment affect the corrosion rate. In the analysis, the vacuum heat-treated sample was found to be more resilient to hydriding at the nucleation and growth stage, exhibiting a reduced number of nucleation points when compared to the as-cast uranium. The work-hardened sample was observed to be more susceptible to H₂ corrosion, displaying

very dissimilar hydriding behavior when compared to the other. Also they concluded vacuum annealing of uranium at a high temperature (550 °C) and for prolonged period (140 h) (prior to surface preparation) produced a relatively stress-free sample where recrystallisation, grain growth and twin boundary reduction was observed.[2]

Rebecca J.L. Welbourn, C.L. Truscotta, M.W.A. Skodab, A. Zarbakhshc, S.M. Clarkea investigated on corrosion and inhibition of copper in hydrocarbon solution on a molecular level.

The authors come up with conclusion that when exposed to a corrosive sulphur solution, the hexadecylamine provides a good corrosion resistance with no change in reflectivity observed within the timescale of the experiment. This is supported by visible observations, SEM and XPS. However, when the hexadecanethiol sample is exposed to corrosive sulphur it does not offer a good resistance, with significant roughening of the surface within 15 min of addition. The reflectivity result is again supported by visible observation, SEM and XPS, which indicate formation of Cu₂S on the surface. Therefore although the adsorbed hexadecylamine layer was not as perfect as the hexadecanethiol layer, it still enabled better corrosion protection.[3]

Z.B. Wang, H.X. Hu, Y.G. Zheng investigated synergistic effects of fluoride and chloride on general corrosion behavior of AISI 316 stainless steel and pure titanium in H₂SO₄ solutions They compared the general corrosion resistance of these two materials to F⁻ and Cl⁻ is and explained by the proposed mechanisms based on XPS analyses. The findings were that both F⁻ and Cl⁻ can accelerate the general corrosion of 316 SS. By contrast, the effects of Cl⁻ on the corrosion of pure Ti depend on the F⁻ concentration. Cl⁻ can decrease the corrosion

potential when pure Ti shows spontaneous passive behavior at lower F⁻ concentrations (0 mM and 0.5 mM) by inhibiting the cathodic process, while no effects can be identified when pure Ti exhibits active-passive behavior at higher F⁻ concentration (5 mM)[4]

Linghui Yang, Yunxiao Wan, Zhenlan Qin, Qunjie Xu, Yulin Min Fabricated and studied corrosion resistance of a graphene-tin oxide composite film on aluminium alloy 6061. The authors concluded that the composite film, whose protection efficiency (η_p) reached 99.7%, can prevent the AA 6061 from corrosion well in a mixed acidic solution of 0.5 M H₂SO₄ and 2 ppm HF with the measurements of Tafel polarization curves and EIS.[5]

L.B. Coelhoa, D. Cossementb, M.-G. Olivier used Benzotriazole and cerium chloride as corrosion inhibitors for AA2024-T3 the investigation is performed on the inhibitive effects provided by benzotriazole (BTA) and cerium chloride (CeCl₃) on 2024-T3 aluminium alloy. Results were assessed, individually and combined, in 0.05 M NaCl electrolytes, by means of Electrochemical

Impedance Spectroscopy (EIS). The results indicated that the combined system offers only limited protection to the alloy, contrary to the outstanding levels of inhibition previously depicted for the Al/Cu model. The EIS study carried out with CeCl₃ on AA2024 was able to demonstrate that high inhibitor concentrations are not necessarily beneficial for corrosion protection over time.[6]

Thuan Dinh Nguyen, Jianqiang Zhang, David J. Young studied Effects of Si, Al and Ti on corrosion of Ni-20Cr and Ni-30Cr alloys in Ar-20CO₂ at 700 °C they concluded that the Ni- 20Cr alloy formed a thick NiO scale and an internal oxidation zone, whereas Ni-30Cr formed a duplex scale of NiO and Cr₂O₃ layers. The Si and Al additions increased the oxidation resistance by forming additional protective layers of SiO₂ or Al₂O₃. Titanium accelerated chromia growth, promoting alloy surface coverage with protective oxide. All alloys formed intergranular Cr-rich carbide precipitates beneath their scales. [7]

F. Zanottoa, V. Grassib, A. Balbob, C. Monticellib, C. Melandric, F. Zucchib studied Effect of brief thermal aging on stress corrosion cracking susceptibility of LDSS 2101 in the presence of chloride and thiosulphate ions.[8]

G.

3. EXPERIMENTATIONS AND DETAIL STUDY

The experiment was designed and performed at sub zero temperature a new corrosion system was designed and developed by M. Esmaily et al is as shown below

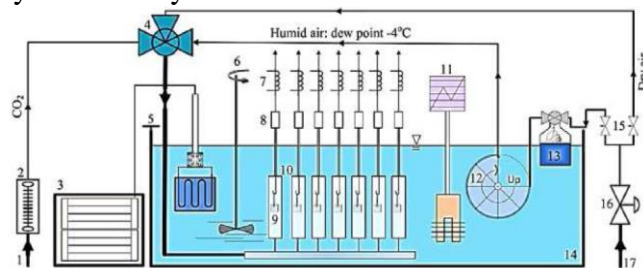


FIGURE 1 Schematic diagram of the exposure chamber for the sub-zero atmospheric corrosion experiment [Referred From: M. Esmaily et al]

Fig 1 shows experimental method develop by M. Esmaily , M. Shahabi-Navid, J.-E. Svensson , M. Halvarsson , L. Nyborg , Y. Cao , L.-G. Johansson. The numbers indicates the parts as (1) CO₂ source, (2) flow meter, (3) dip cooler, (4) mixing chamber, (5) insulation, (6) stirrer, (7) solenoid valves, (8) wash bottles, (9) corrosion samples suspended by nylon string, (10) corrosion chambers, (11) temperature regulator, (12 and 13) humidifiers producing 95% RH air at the exposure temperature (-4C), (14) water +44% ethylene glycol at constant temperature, (15) needle valves, (16) manometer valve (17) dry purified air with a pressure of 6 bars.

Unalloyed Mg (99.97% Mg) was used as reference material. Also the received material was machined and polished. The samples were contaminated with two different amounts of salt, 14 and 70 lg/cm². Care was taken to avoid an uneven distribution of NaCl on the specimen surface by the spraying of the NaCl solution. The quantitative measurements such as gravimetric measurement and Leaching and pickling are performed. Also analytical techniques were used such as X-ray diffraction (XRD), Fourier transform infrared spectroscopy (FTIR), Analytical scanning electron microscope (SEM/EDX) The crystalline corrosion products at -4 and 22 °C were the same. In the absence of both NaCl and CO₂, traces of brucite were identified on 99.97% Mg but not on AM50. In the absence of salt and in the presence of CO₂, no crystalline products were found. NaCl-induced corrosion in the absence of CO₂ resulted in the formation of brucite on both materials. In the case of the alloy, the magnesium aluminum hydroxide meixnerite (Mg₆Al₂(OH)₁₈ · 4.5H₂O) was also identified. In the presence of CO₂ and NaCl, both materials produced three magnesium hydroxy carbonates; H4, H5 and H8.[1]

In the method employed by A. Banos, C.P. Jones, T.B. Scott, A. Banos, C.P. Jones, T.B. Scott three

different samples were taken as cast uranium, thermally annealed uranium. and work hardened uranium. The analytical technique used by secondary ion mass spectrometry (SIMS), FIB milling and rastering – secondary electron (SE) imaging, and EBSD analysis. The results obtained are that the the mass of hydride as well as surface damage, caused per hydride, decreased as we move from a work-hardened to an cast and then a thermally annealed metal surface. Carbide inclusions played a key role in controlling the location of hydride nucleation on all three surfaces, with almost two-thirds of the observed carbide sites acting as nuclei for hydride growth. Cold work-hardening of the metal surface, imparted strain which most quantifiably manifest as an increase in the number of twin boundaries. This had the effect of significantly altering the corrosion behavior of the metal surface [2]

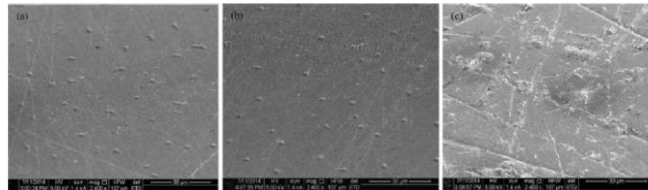


FIGURE 2 Secondary electron (SE) images of Magnox-U hydrided samples showing (a) the as-cast; (b) the thermally annealed and (c) the work-hardened surfaces after partial reaction under 500 mbar (50 kPa) D2 at 190 °C.(Referred From: A. Banos, C.P. Jones, T.B. ScottA. Banos, C.P. Jones)

Plate1: The hydriding parameters of reacted surfaces.(Referred From: A. Banos, C.P. Jones, T.B.ScottA. Banos, C.P. Jones)

The hydriding parameters of all three reacted surfaces.

Sample	Spatial density (hydrides/ mm ²)	Small hydride diameter (µm)	Large hydride diameter (µm)	Percent of hydrides associated with grain/twin boundaries (%)	Percent of carbides accommodating hydride(s) on their peripheries (%)
As-cast	2300 ± 700	4.3 ± 1.5	n/a	-73	-57
Thermally-annealed	1950 ± 600	3.8 ± 1	n/a	-71	-63
Work-hardened	550 ± 500	4 ± 2	16.2 ± 6	-74	-53

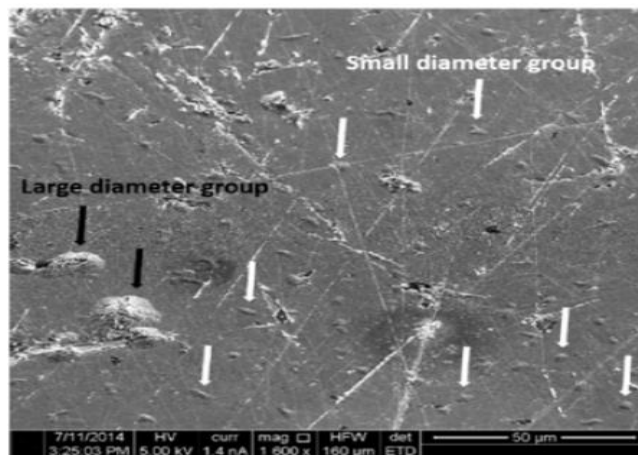


FIGURE 3 Secondary electron image of work hardened surface highlighting abundance of small diameter group on certain areas of sample surface [Coutsey: : A. Banos, C.P. Jones, T.B. ScottA. Banos, C.P. Jones]

Rebecca J.L. Welbourn, C.L. Truscotta, M.W.A. Skodab, A. Zarbakhshc, S.M. Clarkea has performed the analysis for the the behaviour and molecular structure of three organic additives adsorbed from oil onto a copper surface rich in copper (II) oxide is presented. A combination of visible observations, X-ray photoelectron spectroscopy (XPS) and neutron reflection (NR) are used to characterise both the adsorbed layer and underlying copper oxide.The observations are A CuO-rich surface can be induced in a thin film of copper on silicon using a UV/ozone treatment. Authors observed that when exposed to a corrosive sulphur solution, the hexadecylamine provides a good corrosion resistance with no change in reflectivity observed within the timescale of the experiment.

This is supported by visible observations, SEM and XPS.

However, when the hexadecanethiol sample is exposed to corrosive sulphur it does not offer a good resistance, with significant roughening of the surface within 15 min of addition. The reflectivity result is again supported by visible observation, SEM and XPS, which indicate formation of Cu₂S on the surface. Therefore although the adsorbed hexadecylamine layer was not as perfect as the hexadecanethiol layer, it still enabled better corrosion protection. Z.B. Wang, H.X. Hu, Y.G. Zheng Similarly when synergistic effect of fluoride and chloride on general corrosion behavior of AISI 316 stainless steel were observed

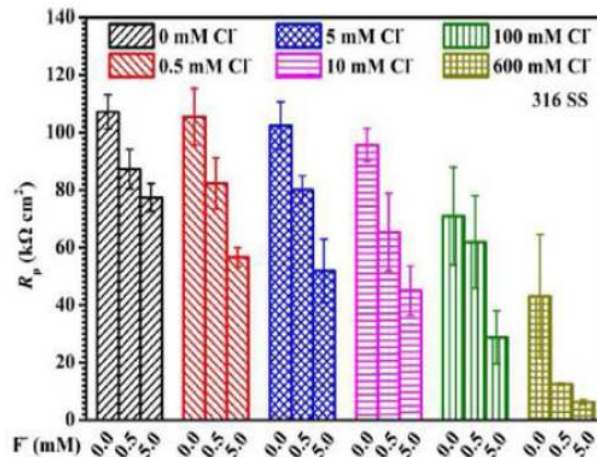


FIGURE 4 Polarization resistance (Rp) of 316 SS obtained by fitting EIS at OCP after 1 hr immersion in H₂SO solution with various content of F⁻ and Cl⁻ (Referred From: Z.B. Wang, H.X. Hu, Y.G. Zheng)

The results of EIS was obtained and plotted as shown in above figure. The synergistic effects of F⁻ and Cl⁻ on the general corrosion resistance of 316 SS and pure Ti are calculated. Negative and positive synergistic effects are found for 316 SS at lower (0.5 mM) and higher (5 mM) F⁻ concentrations, respectively. While only positive synergistic effect is confirmed for pure Ti regardless of F⁻ and Cl⁻ concentrations. These phenomena are explained based on the XPS results that Cl⁻ can facilitate the penetration of F⁻ while F⁻ can inhibit the ingress of Cl⁻ into the films of both 316 SS and pure Ti. Linghui Yang, Yunxiao Wan, Zhenlan Qin, Qunjie Xu, Yulin Min observed corrosion resistance of a graphene-tin oxide composite film on aluminium alloy 6061 . All the samples was tested by traditional three-electrode system and EIS.

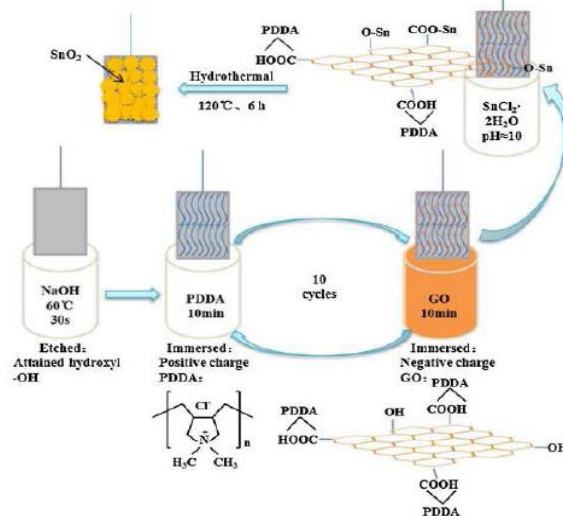


FIGURE 5 Process showing fabrication of composite film on AA 6061 (Referred From: Linghui Yang, Yunxiao Wan, Zhenlan Qin, Qunjie Xu, Yulin Min)

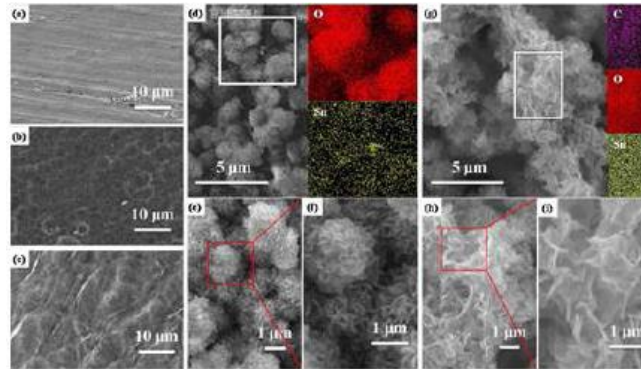


FIGURE 6 SEM images of AA 6061: (a) bare; (b) etched; (c) covered pure graphene film; (d) covered pure SnO₂ film (the inset is element mapping) and (g) covered graphene-SnO₂ composite film (the inset is element mapping). (f) and (i) are expanded views of the red regions of (e) and (h) at different magnifications. (Referred From: Linghui Yang, Yunxiao Wan, Zhenlan Qin, Qunjie Xu, Yulin Min)

The graphene has form a physical barrier layer between the metal and active medium, which prevents the active medium diffusing and permeating effectively. Then, under the common action of the good chemical stability of SnO₂, the surface of the aluminium substrate can be protected. The composite film, whose protection efficiency reached 99.7%, can prevent the AA 6061 from corrosion well in a mixed acidic solution of 0.5 M H₂SO₄ and 2 ppm HF with the measurements of Tafel polarisation curves and EIS.

L.B. Coelhoa, D. Cossementb, M.-G. Oliviera, used Benzotriazole and cerium chloride as corrosion inhibitors for AA2024-T3 . The results were observed by EIS, scanning vibrating electrode technique. They concluded that The inhibitive actions of benzotriazole and cerium chloride were assessed, separately and combined, on AA2024-T3 by means of EIS measurements performed in 0.05 M NaCl reference solution. The results indicated that the combined system offers only limited protection to the alloy, contrary to the outstanding levels of inhibition previously depicted for the Al/Cu model.

Thuan Dinh Nguyen, Jianqiang Zhang, David J. Young tested the Effects of Si, Al and Ti on corrosion of Ni-20Cr and Ni-30Cr alloys in Ar-20CO₂ at higher temperature they found that the Si and Al additions increased the oxidation resistance by forming additional protective layers of SiO₂ or Al₂O₃. Titanium accelerated chromia growth, promoting alloy surface coverage with protective oxide.

All alloys formed intergranular Cr-rich carbide precipitates beneath their scales. Also the conclusion was that additional of Si, Al and Ti significantly improved the oxidation resistance of both Ni-20Cr and Ni-30Cr. The Si-containing alloys formed an additional SiO₂ layer at the scale-alloy interface, effectively reducing Cr₂O₃ growth rate and Cr depletion in the underlying alloy. The most beneficial level is 1% Si. The Al-bearing alloys formed internal, stable Al₂O₃ precipitates at the IOZ-alloy interface, slowing development of the IOZ and the external Ni-rich scale.

Bing Liu, Xinxin Zhang, Xiaorong Zhou, Teruo Hashimoto, Junjie Wang found the corrosion behaviour of machined AA7150-T651 aluminium alloy. It is found that machining operation introduces a near-surface deformed layer, characterized by ultrafine grains and segregation of Mg and Zn at grain boundaries, to the alloy. The near-surface deformed layer is electrochemically more active compared with the bulk alloy, therefore, is preferentially corroded during immersion in an 3.5 wt.% sodium chloride solution acidified to pH 3.2. Also Industrial machining operation introduces a near-surface deformed layer to the AA7150-T651 aluminum alloy. The deformed layer is characterized by ultrafine grains and segregation of alloying elements, magnesium and zinc, at

the grain boundaries. The grain refinement is achieved by continuous dynamic recrystallization during machining. The strengthening precipitates ($MgZn_2$) that are initially present in the AA7150-T651 alloy are dissolved into the aluminum matrix within the near-surface deformed layer due to the relatively high temperature generated within the region immediately beneath the machining tool. The alloying elements, magnesium and zinc, have subsequently segregated at the grain boundaries within the deformed layer.

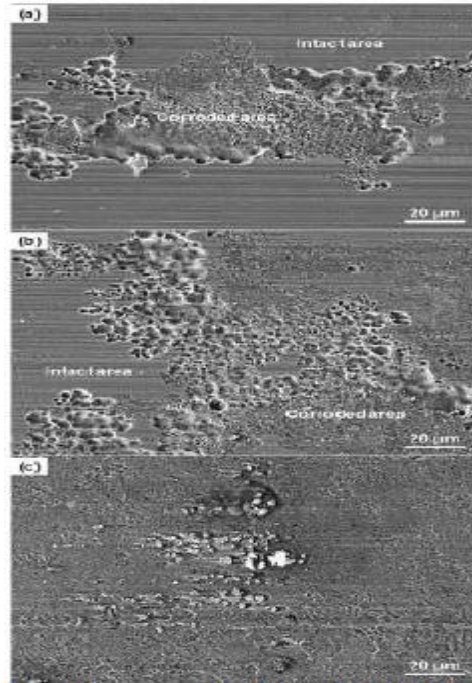


FIGURE 7 Scanning electron micrographs of the machined AA7150-T651 aluminium alloy at different stages during open circuit potential measurement in a 3.5 wt.% sodium chloride solution acidified to pH 3.2 (Referred From: Bing Liu, Xinxin Zhang, Xiaorong Zhou, Teruo Hashimoto, Junjie Wang)

Kenneth Kanayo Alaneme, Sunday Joseph Olusegun, Oluwabunkunmi Tomi Adelowo studied *Hunteria umbellata* seed husk extracts as a corrosion inhibitor on mild steel in acidic solution. The results were obtained by mass loss method, FTIR (Fourier transform infrared spectroscopy) analysis.

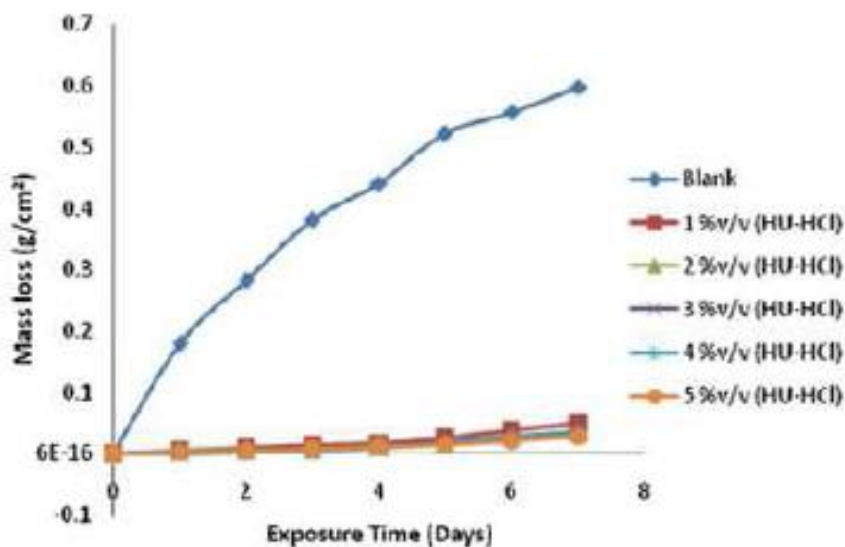


FIGURE 8 Plot of mass loss as a function of time for the corrosion of mild steel in 1 M HCl, in the absence and presence of HCl extract of *Hunteria umbellata* seed husk.[Referred From: Kenneth Kanayo Alaneme, Sunday Joseph Olusegun, Oluwabunkunmi Tomi Adelowo]

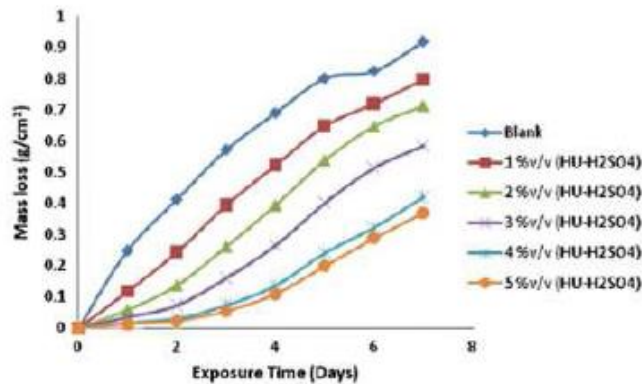


FIGURE 9 Plot of mass loss as a function of time for the corrosion of mild steel in 1 M H₂SO₄, in the absence and presence of H₂SO₄ extract of *Hunteria umbellata* seed husk.[Referred From: Kenneth Kanayo Alaneme, Sunday Joseph Olusegun, Oluwabunkunmi Tomi Adelowo]

The test were also performed on Effect of temperature on corrosion rate and inhibition efficiency of the extract. The important conclusion was The inhibition efficiency was found to increase with increase in extract concentration in the acidic solutions but decreases with increase in temperature.

CONCLUSION

From this paper it can be concluded that as corrosion is serious problems in industries as metal is integral part of day today life. Though complete elimination of corrosion is not possible but it can be reduce to various environments by different methods such as coating, changing process parameters. Also it is concluded that changing microstructure and material characteristics deeply affect corrosion behavior of material. From above paper study it can be seen that proper treatment can reduce corrosion rate considerably so that timely optimized correct corrosion inhibition procedure should be adopted to get effective result

REFERENCES

1. M. Esmaily, M. Shahabi-Navid, J.-E. Svensson, M. Halvarsson, L. Nyborg, Y. Cao, L.-G. Johansson, "Influence of temperature on the atmospheric corrosion of the Mg–Al alloy AM50", *Journal of Corrosion Science*, pp. 420-433, Year 2015
2. A. Banos, C.P. Jones, T.B. Scott, "The effect of work-hardening and thermal annealing on the early stages of the uranium-hydrogen corrosion reaction", *Journal of Corrosion Science*, Year 2017
3. Rebecca J.L. Welbourn, C.L. Truscott, M.W.A. Skoda, A. Zorbakhsh, S.M. Clarke, "Corrosion and inhibition of copper in hydrocarbon solution on a molecular level investigated using neutron reflectometry and XPS", *Journal of Corrosion Science*, Year 2017, pp.68-77
4. Z.B. Wang, H.X. Hu, Y.G. Zheng, "Synergistic effects of fluoride and chloride on general corrosion behavior of AISI 316 stainless steel and pure titanium in H₂SO₄ solutions" *Journal of Corrosion Science*, Year 2018, pp.203-217
5. Linghui Yang, Yunxiao Wan, Zhenlan Qin, Qunjie Xu, Yulin Min, "Fabrication and corrosion resistance of a graphene-tin oxide composite film on aluminium alloy 6061", *Journal of Corrosion Science*, Year 2018, pp.85-94
6. L.B. Coelho, D. Cossement, M.-G. Olivier, "Benzotriazole and cerium chloride as corrosion inhibitors for AA2024-T3: An EIS investigation supported by SVET and ToF-SIMS analysis" *Journal of Corrosion Science*, Year 2018, pp.177-189



7. Thuan Dinh Nguyen, Jianqiang Zhang, David J. Young, “Effects of Si, Al and Ti on corrosion of Ni-20Cr and Ni-30Cr alloys in Ar- 20CO₂ at 700 °C”, Journal of Corrosion Science, Year 2018, pp.161-176
8. F. Zanotto, V. Grassi, A. Balbo, C. Monticelli, C. Melandri, F. Zucchi, “Effect of brief thermal aging on stress corrosion cracking susceptibility of LDSS 2101 in the presence of chloride and thiosulphate ions”, Journal of Corrosion Science, Year 2018, pp.22-30
9. <https://www.thebalance.com/corrosion-revention-2340000>
10. <https://en.wikipedia.org/wiki/Corrosion>
11. R. Winston Revie, Herbert H. Uhling, Corrosion and Corrosion Control, An Introduction to Corrosion Science and Engineering, 4th edition, A John Wiley and Sons, Inc. Publications (2008)